High switching frequency CCM PFC operation with TRENCHSTOP™ 5 WR5 IGBT discrete

Validity of TRENCHSTOP™5 WR5 IGBT in high switching frequency operation in CCM (continuous conduction mode) PFC (power factor correction)

About this document

This application note demonstrates the performances of TRENCHSTOP™ 5 WR5 IGBT in high switching frequency and its application benefits CCM PFC for major home appliances.

Scope and purpose

This document aims to help PFC design engineers in home appliance applications who want to increase switching frequency to achieve the inductor on the board to minimize the system form factor and lower the system cost.

Intended audience

Design engineers of major home appliances power systems, application engineers, students

Table of contents

About this document **1**
Table of contents **1**
1 Introduction **2**
2 PFC for major home appliances **3**
3 Power loss analysis of IGBT in CCM PFC **5**
3.1 Conduction loss calculation 5
3.2 Switching loss calculation 6
3.3 Power loss analysis of Infineon's TRENCHSTOP™ 5 WR5 IGBT 6
3.3.1 Electrical characteristics 7
3.3.2 Power loss simulation 11
4 Experimental results **13**
4.1 System description 13
4.2 Efficiency and thermal performance evaluation 14
4.3 EMI performance evaluation 15
4.4 SC immunity of IKW40N65WR5 17
5 Conclusion **20**
6 References **21**
Revision history **22**

1 Introduction

In modern society, as the energy consumed by home appliances is steadily increasing, it has become more and more important to maintain a high-power factor (PF) when using these appliances. Air conditioners in particular are the most power-consuming home appliance; and for their design, a power factor correction (PFC) is mandatory. In general, air conditioner applications have a power rating of 1.8 kW or higher, thereby IGBTs are the most appropriate switching device considering the cost-performance ratio. Although IGBTs show much lower conduction loss than power MOSFETs, slower switching speed and tail current characteristics of IGBTs have been limited to increase in the switching frequency. In general, the proper switching frequency of IGBTs has been considered to be far below 60 kHz. In PFC systems, lower switching frequency increases the size of the boost inductor, which cannot then be placed on the main circuit board. In this case, the cost of the inductor is inevitably high, and the form factor of the system will be limited. Moreover, the high risk of short-circuit incidents that may occur during installation or maintenance processes requires short-circuit rated IGBTs for safety. In order to ensure the protection of IGBTs from short-circuit (SC) conditions, a SC rated IGBT is required. In this case, the IGBT has to cope with certain disadvantages in terms of $V_{ce(sat)}$ and switching performance in order to ensure short-circuit immunity. Thus, the demand for integrating the PFC inductor on the main board by increasing switching frequency continues to increase, to minimize the system form factor, to reduce the cost of inductor, and to use high performance IGBTs.

2 PFC for major home appliances

The boost converter in Figure 1 is the most common topology for active PFC circuits, as it can maintain continuous input current, which is most beneficial in terms of lower harmonics and less EMI filter requirements. For PFC in major home appliances especially, CCM (continuous conduction mode) is used because of easier EMI filter design owing to fewer harmonics, lower conduction loss due to lower RMS current, and lower turn-off loss.

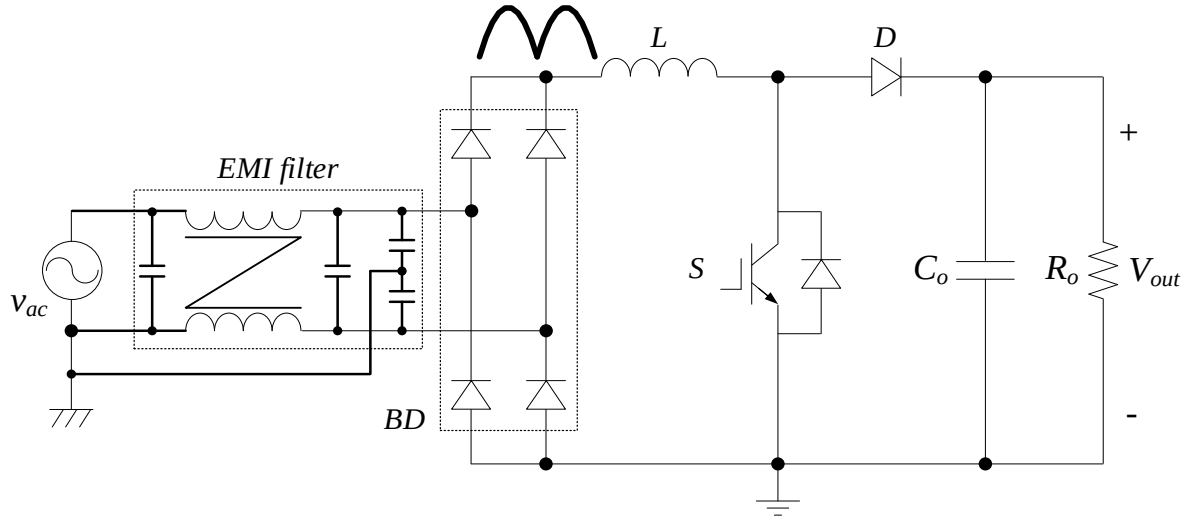


Figure 1 PFC circuit with boost converter topology

The inductor current ripple reaches its maximum value when the instantaneous value of AC input is equal to $V_{out}/2$. However, at high power CCM PFC, the minimum AC input voltage, V_{ac_min}, is approximately at least 180V and its peak value is always higher than $V_{out}/2$. The required inductance, L, for CCM PFC is obtained by using the follow equations.

$$\Delta I_L = \frac{1}{L}\int_0^{DT_s} \sqrt{2}V_{ac_min}(t)dt = \frac{V_{out}}{L \cdot f_{sw}}\left(\frac{V_{out} - \sqrt{2}V_{ac_min}}{V_{out}}\right) \quad (1)$$

$$L \geq \frac{{V_{ac_min}}^2}{\%ripple \cdot P_{out} \cdot f_{sw}}\left(\frac{V_{out} - \sqrt{2}V_{ac_min}}{V_{out}}\right) \quad (2)$$

where, $\%\text{ripple} = \Delta I_L / I_{L_pk}$, and $I_{L_pk} = \sqrt{2}P_{out}/V_{ac_min}$.
As the value of inductance becomes larger, the switching ripple current will become smaller. However, a bulkier inductor is required and this can result in an increase in cost. Meanwhile, the PFC can maintain CCM operation as long as $\Delta I_L/2$ is less than I_L; thereby, it is necessary to choose the optimal inductance in terms of cost and performance. The required inductance for CCM PFC in accordance with the switching frequency is indicated in Figure 2. Figure 2 shows that the required inductance becomes significantly smaller as switching frequency increases. When it exceeds 60 kHz, it will become small enough to be placed on the main board.
The capacitance of the PFC output capacitor is independent of the switching frequency, but needs to meet both hold-up time requirement (when brownout occurs) and low-frequency ripple voltage requirements as shown in Equation 2 and Equation 3.

$$C_{out} \geq \frac{2P_{out} \cdot t_{hold-up}}{{V_{out}}^2 - {V_{out_min}}^2} \quad (3)$$

$$C_{out} \geq \frac{P_{out}}{2\pi \cdot f_{ac} \cdot \Delta V_{out} \cdot V_{out}} \quad (4)$$

In general, the hold-up time is defined as one cycle of line frequency, i.e it is greater than than 20 ms at 50 Hz or 16 ms at 60 Hz. Meanwhile, the ripple voltage requirement is defined by the customer, and is determined at the range approximately 10-20 V.

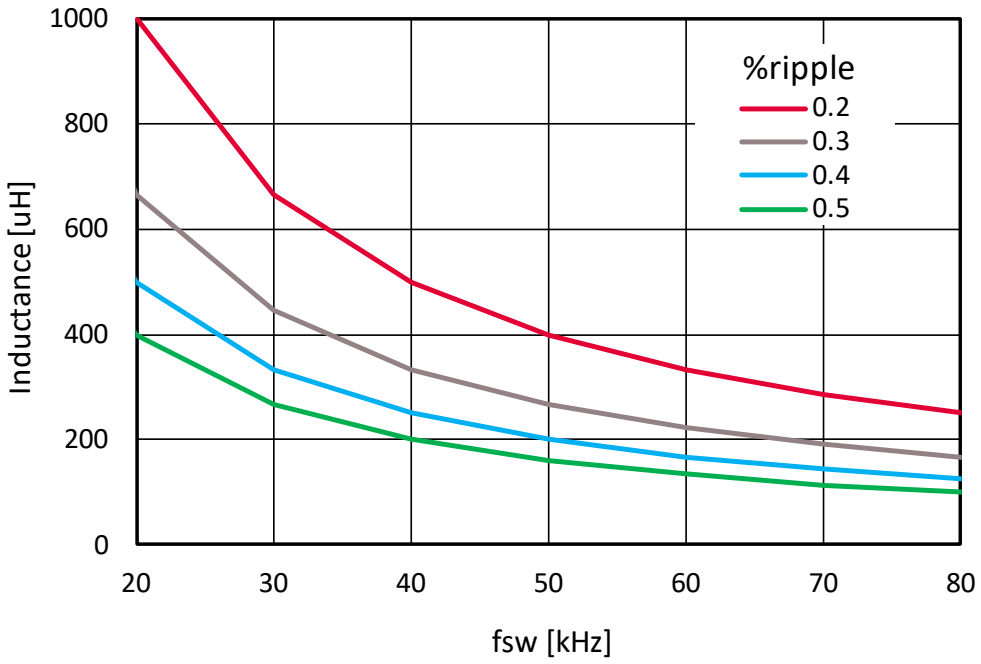


Figure 2 Inductance vs. switching frequency for P_{out}=2.5 kW, and V_{ac_min}=180 V

3 Power loss analysis of IGBT in CCM PFC

In order to verify the validity of Infineon's TRENCHSTOP™ 5 WR5 IGBT, power loss calculation methods are described as follows.

3.1 Conduction loss calculation

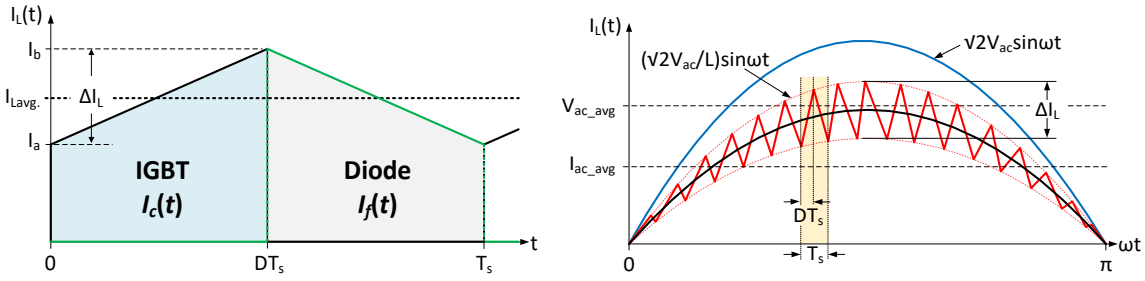


Figure 3 IGBT and FRD waveforms of PFC in CCM operation

Figure 3 indicates the IGBT and FRD waveforms of PFC in CCM operation.
In CCM boost-converter operation, the voltage drops at IGBT, V_{ce_sat} and FRD, V_F can be indicated as follows:

$$V_{ce_{sat}}(t) = r_{ce}\, I_c(t) + V_{ce0} \tag{5}$$

$$V_F(t) = r_F\, I_c(t) + V_{F0} \tag{6}$$

where, $I_c(t) = I_a + \frac{I_b - I_a}{DT_s} t$

Therefore, the conduction loss of the IGBT for a single period can be calculated by

$$\begin{aligned} P_{IGBT_CON} &= \frac{1}{T_s}\int_0^{DT_s} V_{ce}(t) \times I_c(t)dt \\ &= \frac{1}{T_s}\int_0^{DT_s} \left\{ V_{ce0}\left(I_a + \frac{I_b - I_a}{DT_s}t\right) + r_{ce}\left(I_a + \frac{I_b - I_a}{DT_s}t\right)^2 \right\} dt \\ &= D\left\{ \frac{V_{ce0}}{2}(I_a + I_b) + \frac{r_{ce}}{3}\left({I_a}^2 + I_a I_b + {I_b}^2\right) \right\} \end{aligned} \tag{7}$$

However, small amounts of ripple current do not contribute much to RMS (root mean square) value, as it makes the calculation more complicated. Thus, the ripple component can be neglected, and equation 7 can be simply expressed as

$$P_{IGBT_CON} = D(t)\left(V_{ce0} i_L(t) + r_{ce} {i_L}^2(t)\right) \tag{8}$$

Meanwhile, since the input voltage is sinusoidal, $D(t)$ and $i_L(t)$ are expressed as

$$D(t) = \frac{V_{out} - \sqrt{2}V_{ac} sin\omega t}{V_{out}} \tag{9}$$

$$\begin{aligned} i_L(t) &= \sqrt{2} I_{ac} sin\omega t \\ &= \frac{\sqrt{2} P_{out}}{\eta V_{ac}}\, sin\omega t \end{aligned} \tag{10}$$

Therefore, the average conduction loss of the IGBT can be derived by

$$< P_{IGBT_CON} >= \frac{1}{\pi}\int_0^{\pi}\left(\frac{V_{out}-\sqrt{2}V_{ac}sin\omega t}{V_{out}}\right)\left(\sqrt{2}V_{ce0}I_{ac}sin\omega t + 2r_{ce}{I_{ac}}^2 sin^2\omega t\right)d\omega t$$
$$= V_{ce0}I_{ac}\left(\frac{2\sqrt{2}}{\pi}-\frac{V_{ac}}{V_{out}}\right)+r_{ce}{I_{ac}}^2\left(1-\frac{8\sqrt{2}V_{ac}}{3\pi V_{out}}\right)[\mathrm{W}] \quad (11)$$

In the same way, the conduction loss of the diode is obtained by

$$< P_{FRD_CON} >= \frac{1}{\pi}\int_0^{\pi}-\frac{\sqrt{2}V_{ac}sin\omega t}{V_{out}}\left(\sqrt{2}V_{F0}I_{ac}sin\omega t + 2r_F{I_{ac}}^2 sin^2\omega t\right)d\omega t$$
$$= \frac{V_{ac}}{V_{out}}\left(V_{F0}I_{ac}+\frac{8\sqrt{2}}{3\pi}r_F{I_{ac}}^2\right)[\mathrm{W}] \quad (12)$$

3.2 Switching loss calculation

The conduction loss of IGBT can be obtained with relatively accurate values from a datasheet. On the other hand, it is impossible to derive the reliable switching loss of an IGBT with datasheet parameters alone. In particular, turn-on loss is significantly affected by the performance of rectifier diodes. However, if the switching energy at high temperatures (generally @ 100°C) is predefined in accordance with the gate resistance value and the level of switching current when combined with a certain diode, switching losses of IGBT can be easily calculated using the equation below.

$$P_{on} = f_{sw}\cdot I_{on_{avg}}\cdot E_{on_factor}\cdot R_{g_on_factor} \quad (13)$$

$$P_{off} = f_{sw}\cdot I_{off_{avg}}\cdot E_{off_factor}\cdot R_{g_off_factor} \quad (14)$$

Additionally, the switching loss of diode can be simplified by

$$P_{D_sw} = \frac{1}{2}V_{out}\cdot Q_c\cdot f_{sw} \quad (15)$$

3.3 Power loss analysis of Infineon's TRENCHSTOP™ 5 WR5 IGBT

In the boost PFC circuit in Figure 1, the potential at the IGBT collector is always higher than the potential at the IGBT emitter under all conditions. Therefore, the anti-parallel diode of the switch device should not be conducted in normal operation, except for a very small resonant current when the PFC operates in CrCM (critical conduction mode). Therefore, the performance requirement of anti-parallel diodes is not that high, this diode needs to protect the IGBT only for abnormal conditions. Meanwhile, as the demand for higher switching frequency increases in major home appliances, the switching performance of IGBTs is becoming increasingly important.

Infineon's TRENCHSTOP™ 5 WR5 IGBT with monolithic anti-parallel diodes, namely reverse conducting (RC) IGBTs, is shown in Figure 4. The RC IGBT concept is that N+ regions are partially implanted into the P-collector layer that forms intrinsic P-N diodes allowing the reverse current to flow without a co-pack diode. This IGBT concept is suitable for boost PFC applications, for which high-performance co-pack diode is not required. This IGBT family offers the best-in-class performance in terms of both conduction and switching behaviors when combined with a SiC diode, and it allows high switching frequency operation beyond 60 kHz.

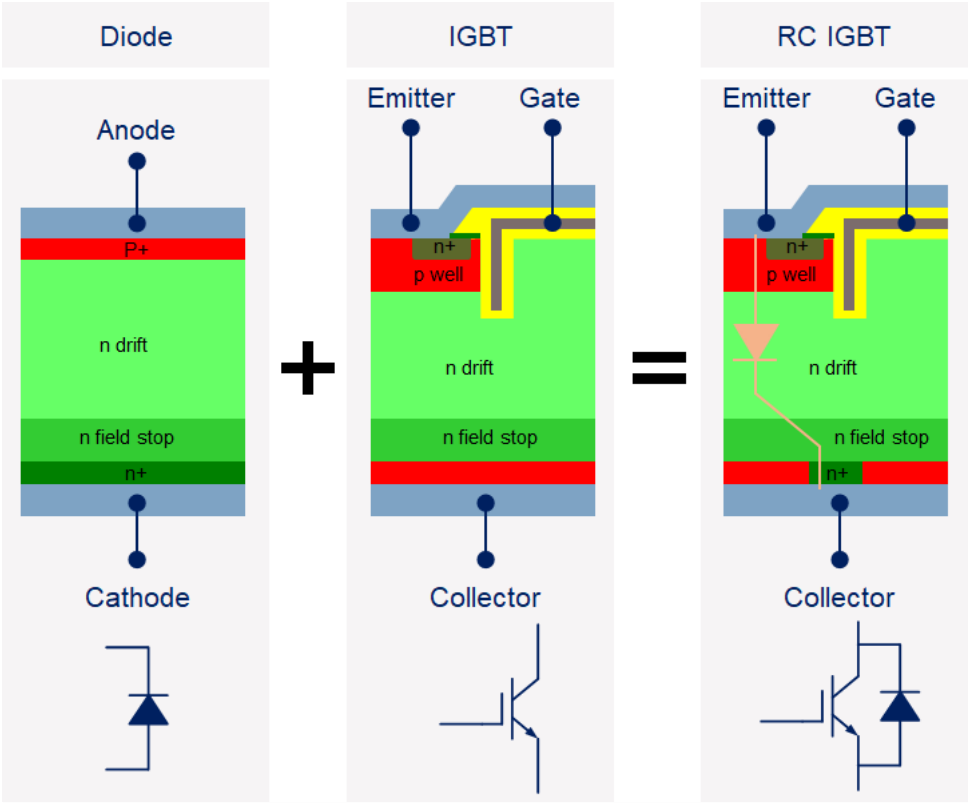
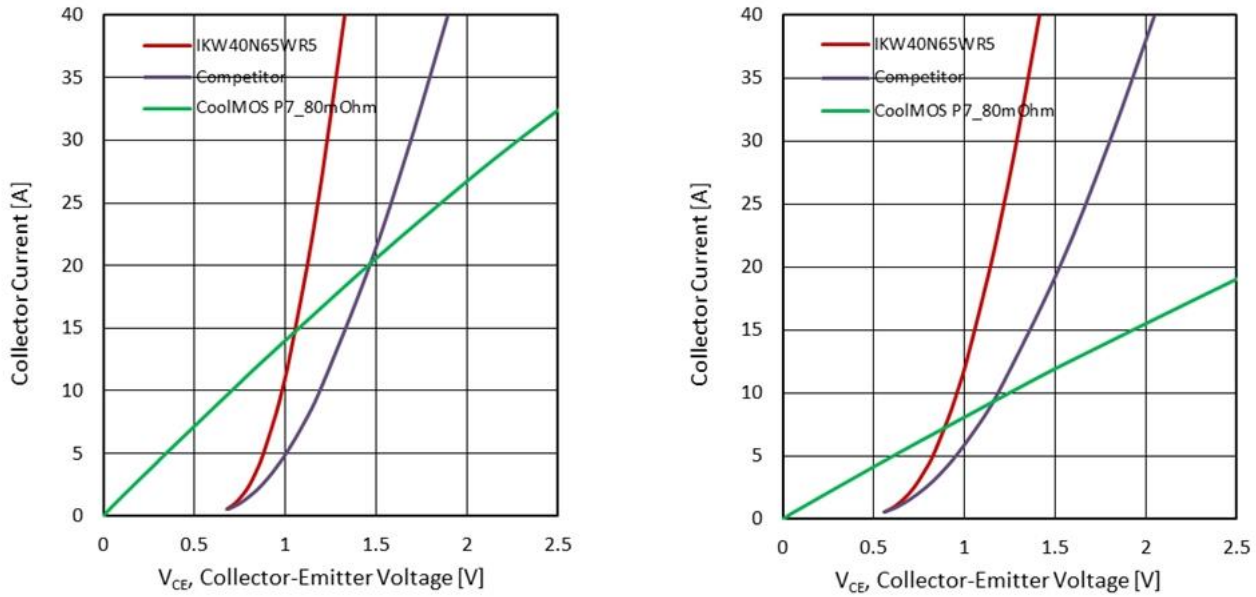


Figure 4 **TRENCHSTOP™ 5 WR5 IGBT using reverse conducting (RC) IGBT concept**

3.3.1 Electrical characteristics

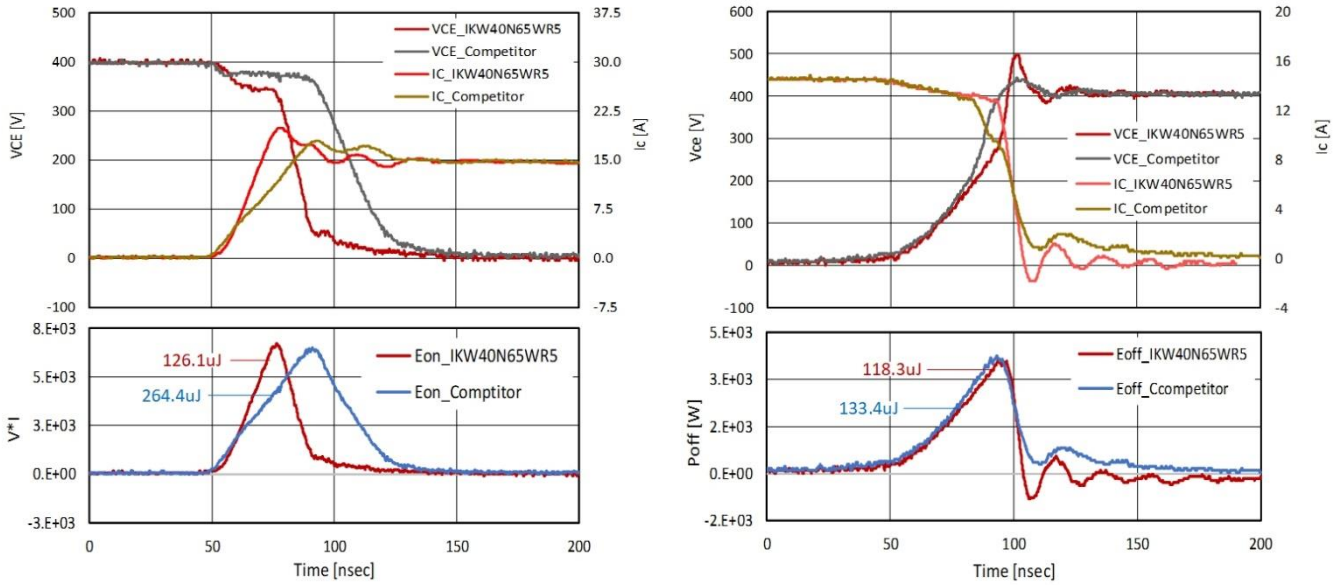
In order to verify the validity of TRENCHSTOP™ 5 WR5 IGBT in high switching frequency operation, the IKW40N65WR5 was chosen, and the electrical characteristics with CoolMOS™ P7 MOSFET of the equivalent rating were compared. Figure 5 shows the static characteristics' comparison between IKW40N65WR5 and an 80 mΩ CoolMOS™ P7 MOSFET. As shown in Figure 5, at low current, the CoolMOS™ P7 MOSFET should be more advantageous than the IGBT. However, in the case of CoolMOS™ P7 MOSFET, the R_{DS_on} increases rapidly as the junction temperature increases, while the variation in voltage drop of the IGBT in accordance with its junction temperature is insignificant. Therefore, as the output power increases and the junction temperature increases, the IGBT becomes more advantageous. Given the output characteristics in Figure 5 (b), IKW40N65WR5 under T_j=100°C conditions has superior performance over the 80 mΩ CoolMOS™ P7 MOSFET when the current is 7-8 A or higher.



(a) Output characteristics @ 25°C (b) Output characteristics @ 100°C

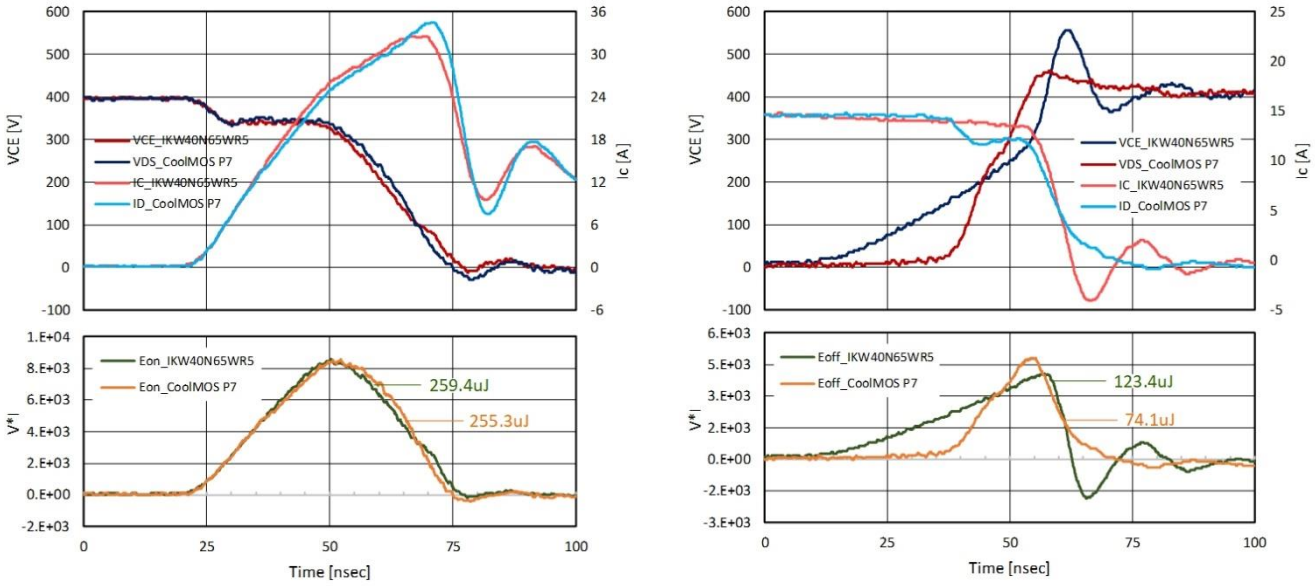
Figure 5 Output characteristics comparison

In order to validate the TRENCHSTOP™ 5 WR5 IGBT in high-switching frequency and high-power operation, a double-pulse test was carried out assuming operating conditions of input voltage 180 V, 2.5 kW CCM PFC, and RMS current of approximately 14.5A.



(a) Turn-on (b) Turn-off

Figure 6 Switching comparison between TRENCHSTOP™ 5 WR5 IGBT and competitor's highest performing IGBT with 20 A SiC diode



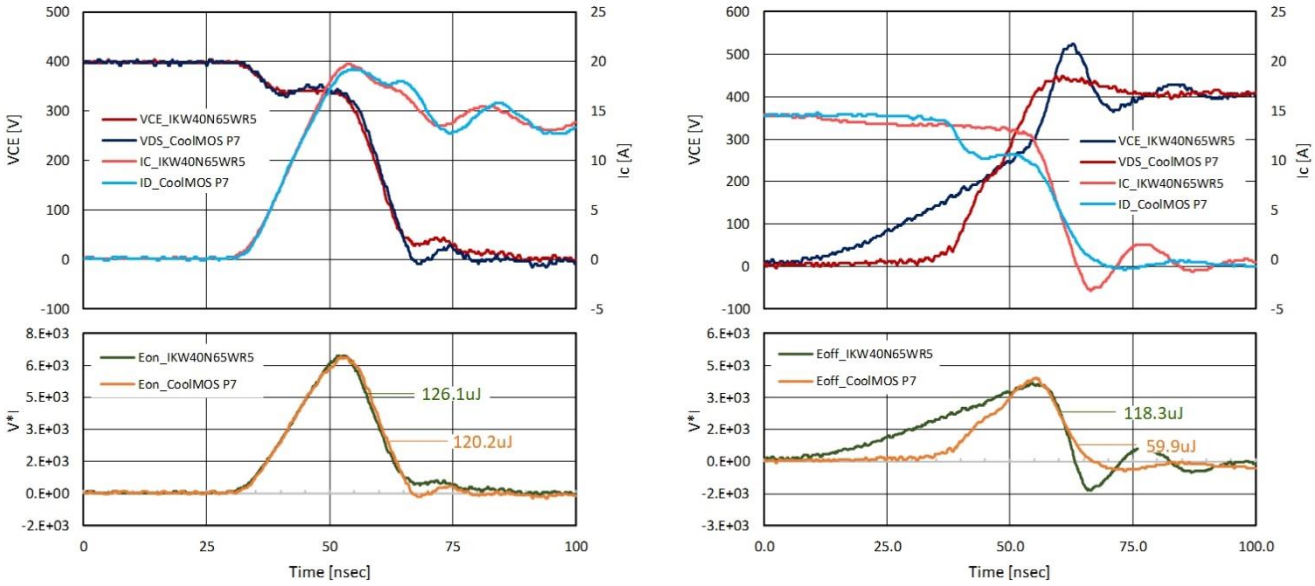
(a) Turn-on (b) Turn-off

Figure 7 Switching comparison between TRENCHSTOP™ 5 WR5 IGBT and CoolMOS™ P7 MOSFET with 30 A Rapid 1 diode

Figure 6 shows the switching performance comparison between IKW40N65WR5 and a competitor's highest performing IGBT combined with 20A SiC diode. As shown in Figure 6, the competitor's IGBT has 2.1 times higher E_{on} and 13.4 % higher E_{off} than IKW40N65WR5. Considering the inferior switching performance as well as higher V_{ce_sat} of the competitor, it is easy to predict that the competitor product will not be suitable for high switching frequency operation.

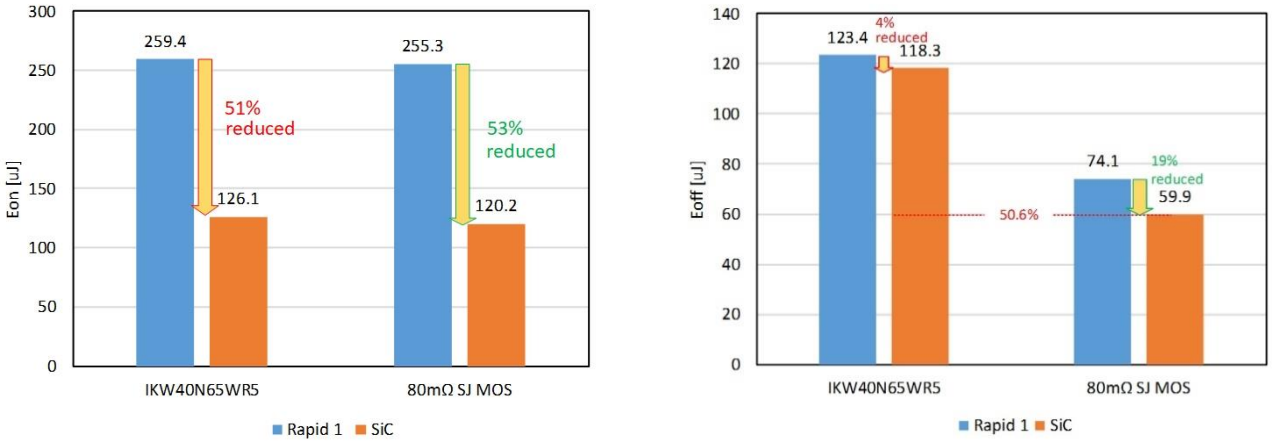
Figure 7 shows the switching test results of IKW40N65WR5 and 80 mΩ CoolMOS™ P7 MOSFET combined with 30 A Si diode. Since the reverse recovery current of the boost diode is extremely high when the devices are turned on instantly, it significantly affects the turn-on energies of both devices, which are much higher than their turn-off energies. The E_{on} of IKW40N65WR5 and 80 mΩ CoolMOS™ P7 MOSFET are 259 µJ and 255.3 µJ, respectively, while the E_{off} is 123.4 µJ and 74.1 µJ, respectively.

Meanwhile, it is remarkable that the turn-on energy of the TRENCHSTOP™ 5 WR5 IGBT was measured to be similar to the equivalent CoolMOS™ P7 MOSFET. Nevertheless, neither device is suitable for high-power and high switching frequency applications with Si diodes due to their extremely high switching energy.



(a) Turn-on (b) Turn-off

Figure 8 Switching comparison between TRENCHSTOP™ 5 WR5 IGBT and CoolMOS™ P7 MOSFET with 20 A SiC diode



(a) E_{on} (b) E_{off}

Figure 9 Effect from SiC diode in CCM PFC

Figure 8 shows the switching performance comparison between IKW40N65WR5 and 80 mΩ CoolMOS™ P7 MOSFET combined with 20 A SiC diode, which well demonstrates the effectiveness of the SiC diode. At turn-on mode, the reverse-recovery current for both devices is much lower than when they are combined with a Si diode. As a result, the turn-on energy for both devices also become significantly smaller than the turn-on energy combined with the Si diode. The E_{on} of IKW40N65WR5, and 80 mΩ CoolMOS™ P7 MOSFET are 126.1 µJ and 120.2 µJ, respectively. The turn-off energies of both devices are not as significant as the turn-on energy improvement. The E_{off} of IKW40N60WR5 and 80 mΩ CoolMOS™ P7 MOSFET are 118.3 µJ and 59.9 µJ, respectively.

Figure 9 well demonstrates how much switching energy can be improved. By combining with a SiC diode, the turn-on energy of IKW40N65WR5 and 80 mΩ CoolMOS™ P7 MOSFET are improved by 51% and 53%, respectively.

3.3.2 Power loss simulation

A power loss simulation was carried out to estimate the validity of TRENCHSTOP™ 5 WR5 IGBT in high switching frequency operations. Table 1 shows the key input parameters for the simulation and its corresponding calculated values, and the loss simulation results from them are given in Table 2 where the switching frequency of 60 kHz is applied. The coefficients given in Table 2 are based on the measured data and can be used to estimate E_{on} and E_{off} at V_{ce}=400V and T_c=100°C, allowing comparison of losses in WR5 and P7 at varied load conditions and R_g values. The coefficients E_{on_factor} and E_{off_factor} is the gradient of the approximated linear curves of the measured switching energies as a function of device current. In addition, the coefficients of the linear equation E_{sw} vs. R_g, normalized to E_{on} and E_{off} values at a given current are also obtained by curve fitting to the measured switching energies as a function of gate resistance.

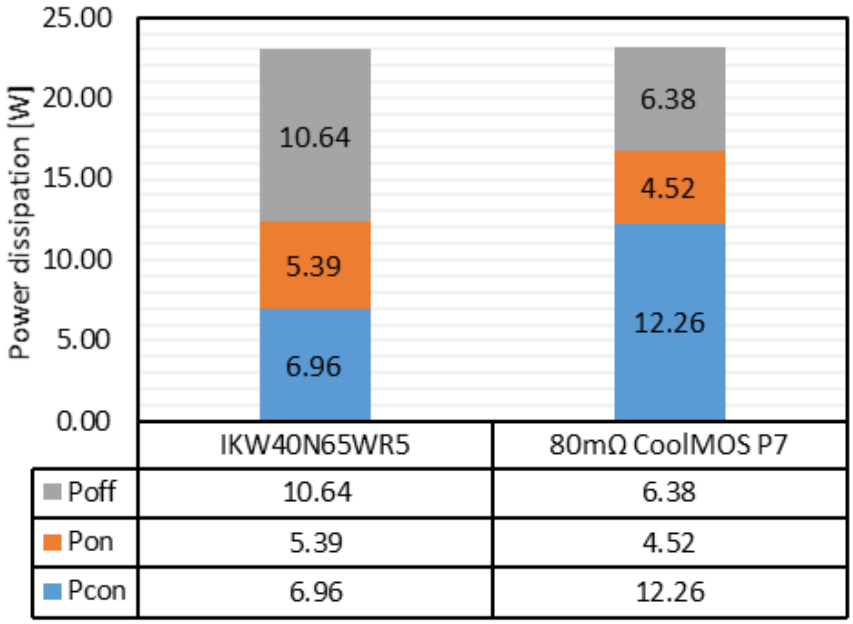
Table 1 Loss simulation parameters 1

Input parameter	Value	Unit	Calculated value	Value	Unit
P_{out}	2500	W	P_{in}	2577.3	W
f_{sw}	60	kHz	$D_{_avg}$	0.55	
V_{in_min}	180	Vac	V_{in_avg}	162.1	V
V_{out}	400	Vdc	I_{in_rms}	14.3	A
Eff.	0.97		I_{in_avg}	12.9	A
R_{g_on}	15	Ω	I_{in_pk}	20.2	A
R_{g_off}	10	Ω	I_{a_avg}	11.6	A
Delta I	0.2		I_{b_avg}	14.2	A

Table 2 Loss simulation parameters 2

Device	$V_{ce0@100°C}$ [V]	$R_{ce@100°C}$ [Ω]	$E_{on_Factor@100°C}$ [µJ]	$E_{off_factor@100°C}$ [µJ]	$R_{g_on_factor@100°C}$	$R_{g_off_factor@100°C}$	P_{con} [W]	P_{on} [W]	P_{off} [W]	P_{tot} [W]
IKW40N65WR5	0.67	0.028	9.7E-06*I_{on}	14.2E-06*I_{off}	0.026R_g + 0.41	0.020R_g + 0.71	**6.96**	**5.39**	**10.64**	**22.99**
80mΩ CoolMOS P7	0	0.130	8.42E-06*I_{on}	10.7E-06*I_{off}	0.011R_g + 0.59	0.03R_g + 0.42	**12.26**	**4.52**	**6.38**	**23.16**

The summarized loss analysis results are described in Figure 10. The simulation result shows that IKW40N65WR5 will perform superior to 80 mΩ CoolMOS™ P7 MOSFET at the switching frequency of 60 kHz, a frequency high enough to have the boost inductor installed on the main board. In the case of IKW40N65WR5, its conduction loss at high power (2.5 kW) & high switching frequency is expected to be only about 30% -35%; the remaining 65% -70% is expected to be switching losses. In the case of 80 mΩ CoolMOS™ P7 MOSFET on the other hand, the conduction loss is expected to be about twice that of IKW40N65WR5, while its switching loss is smaller than that of IKW40N65WR5.



	IKW40N65WR5	80mΩ CoolMOS P7
Poff	10.64	6.38
Pon	5.39	4.52
Pcon	6.96	12.26

Figure 10 Loss calculation result at 60 kHz

4 Experimental results

4.1 System description

In order to validate the devices for high switching frequency operation, an experiment using 2.5 kW CCM PFC in Figure 11 was carried out. The system conditions and tested devices are as follows:

- P_{out}: 250 W-2500 W
- V_{in}: AC 180/230 V-50 Hz
- V_{out}: 400 V

Table 3 Tested devices and conditions

Diode	IGBT	30kHz	60kHz	Remark
IDW30C65D1 (30 A Si Rapid 1 diode)	IKW40N60H3	◯		R_g=20 Ω
	IKW40N65WR5	◯		
20A SiC Diode IDW20G65C2 (20 A SiC diode)	IKW40N65WR5		◯	R_g=10 Ω
	Competitor's highest performing part		◯	
	80 mΩ CoolMOS™ P7 MOSFET		◯	

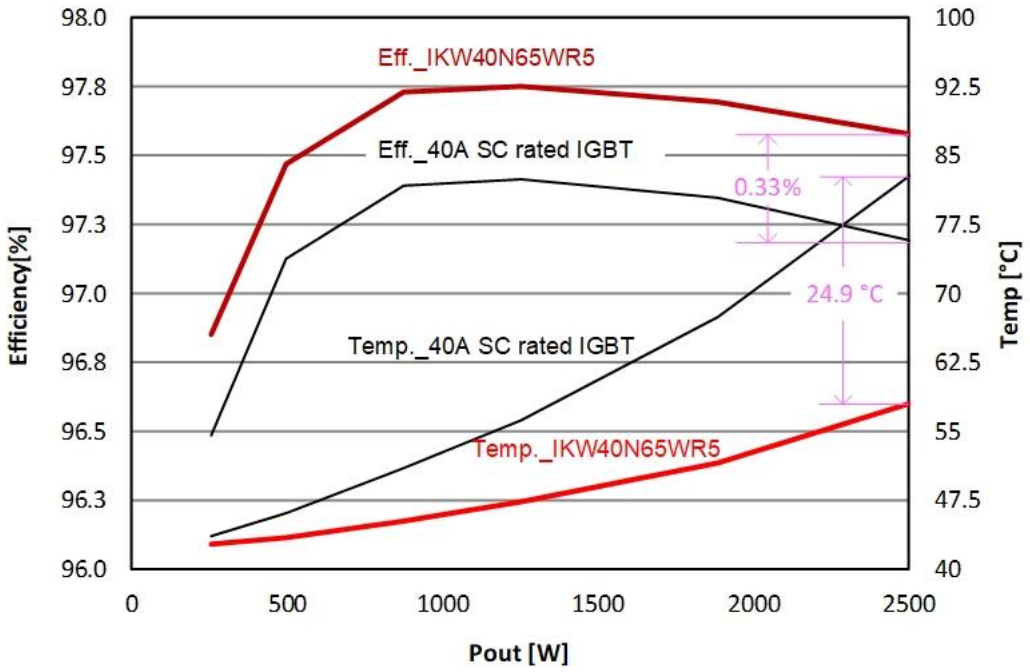


Figure 11 Test setup: 2.5 kW CCM PFC

4.2 Efficiency and thermal performance evaluation

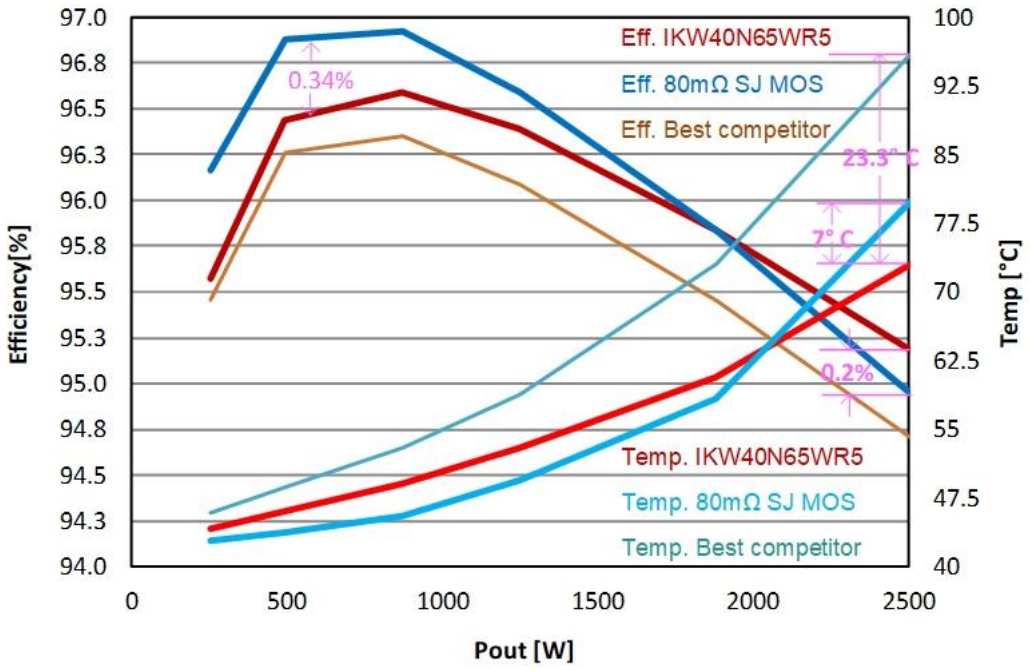
Figure 12 shows the results of measuring the efficiency and thermal performance of IKW40N65WR5 and a conventional SC rated IGBT, IKW40N60H3 at 30 kHz switching frequency conditions. The TRENCHSTOP™ 5 WR5 IGBT is a device that maximizes performance instead of guaranteeing a SCWT (short-circuit withstand time), and is far superior to IKW40N60H3 that has a SCWT of 5 µsec. The efficiency difference between the two devices is up to 0.33 %, and the temperature difference at the front side of package is about 25°C respectively, which means the conventional SC rated IGBT cannot be considered for high switching frequency operation despite its high reliability.

In Figure 13, IKW40N65WR5, 80 mΩ CoolMOS™ P7 MOSFET, and a competitor's highest performing IGBT are compared in terms of efficiency and thermal performance under the switching frequency of 60 kHz. The results show that IKW40N65WR5 overwhelms the competitor's IGBT, both in terms of efficiency and thermal performance over the entire load condition. Between IKW40N65WR5 and the competitor, the maximum temperature gap is more than 23°C and the efficiency gap is about 0.3 % at the maximum load. In addition, IKW40N65WR5 shows better thermal and efficiency performance than the equivalent CoolMOS™ P7 MOSFET at approximately 2 kW and above, while the equivalent CoolMOS™ P7 MOSFET shows slightly better performance in the low to mid-load range.



IKW40N65WR5 vs. 40 A SC rated IGBT

Figure 12 Efficiency & thermal performance test result @ f_{sw}=30 kHz



IKW40N65WR5 vs. Competitor's best performing 40 A IGBT & 80 mΩ CoolMOS™ P7

Figure 13 Efficiency & thermal performance test result @ f_{sw}=60 kHz

The above experimental results are relatively good as seen in the loss simulation results in 2.3.2. From the results in Fig. 13, CoolMOS™ P7 MOSFET would be ideal for light load conditions, on the other hand, for major appliances such as air conditioners where full load conditions are very important, TRENCHSTOP™ 5 WR5 IGBT is clearly the best choice considering cost as well as performance.

4.3 EMI performance evaluation

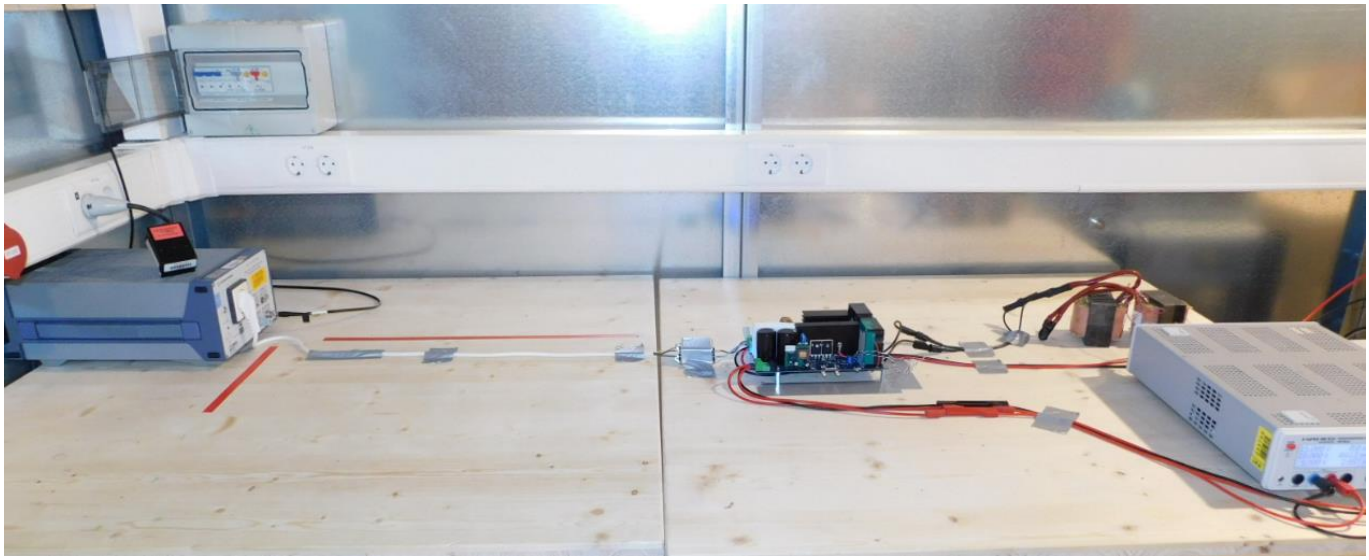
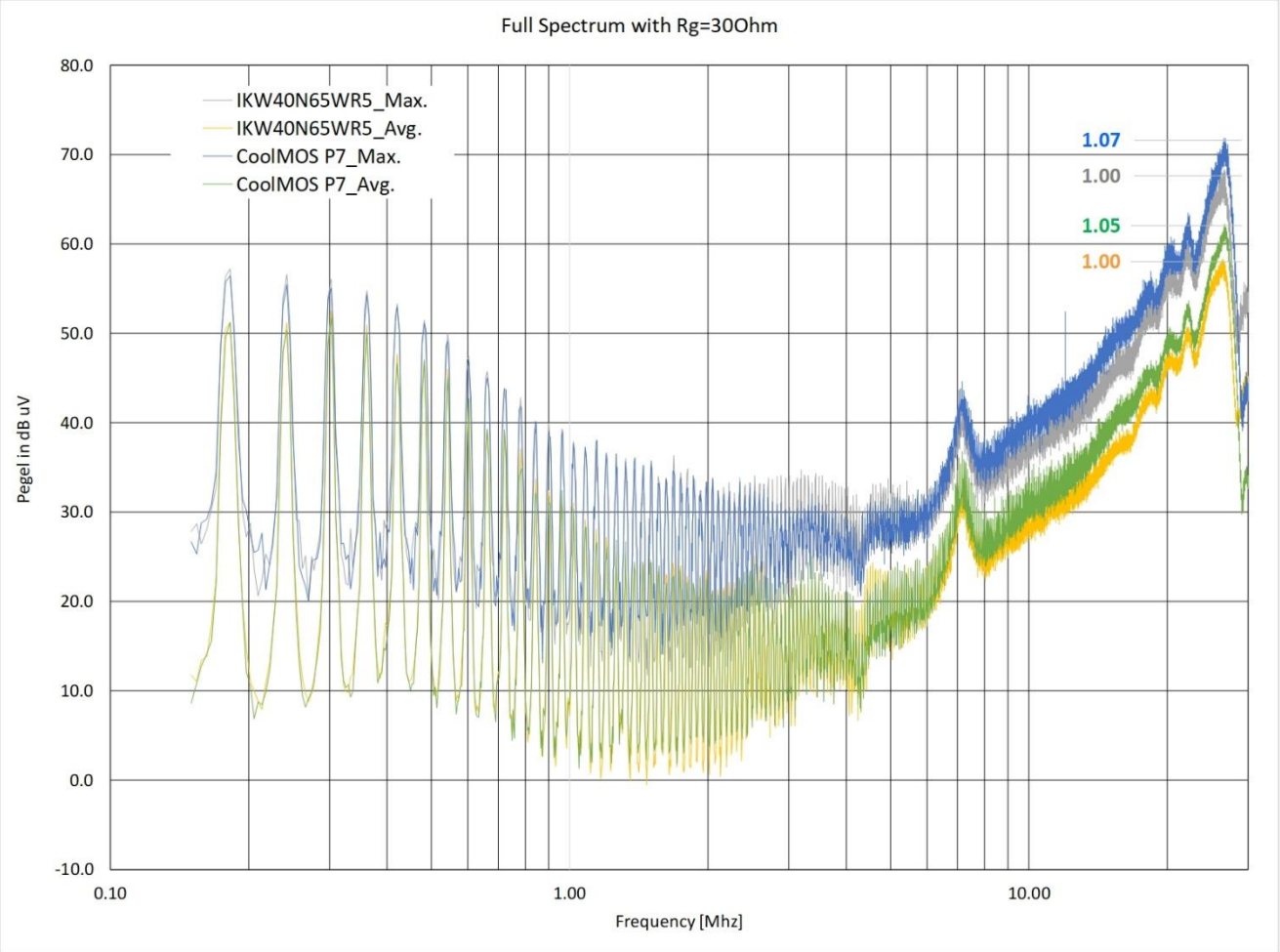


Figure 14 Conduction EMI test set-up and conditions

Besides the efficiency and the thermal performance, EMI characteristics are also considered a very important factor in switching devices for MHA applications. EMI performance is determined by various factors such as dv/dt, di/dt, gate resistance, EMI filter design and so on, thereby its improvement can vary from system to system. However, EMI characteristics of each device can be compared by means of testing under the exact same conditions. The experimental set-up and conditions for comparing EMI performance of devices is displayed in Figure 14. Figure 15 shows the EMI characteristics of IKW40N65WR5 and 80 mΩ CoolMOS™ P7 MOSFET combined with 20 A SiC diode. The result shows that the EMI level of IKW40N65WR5 is lower than that of the CoolMOS™ P7 MOSFET.

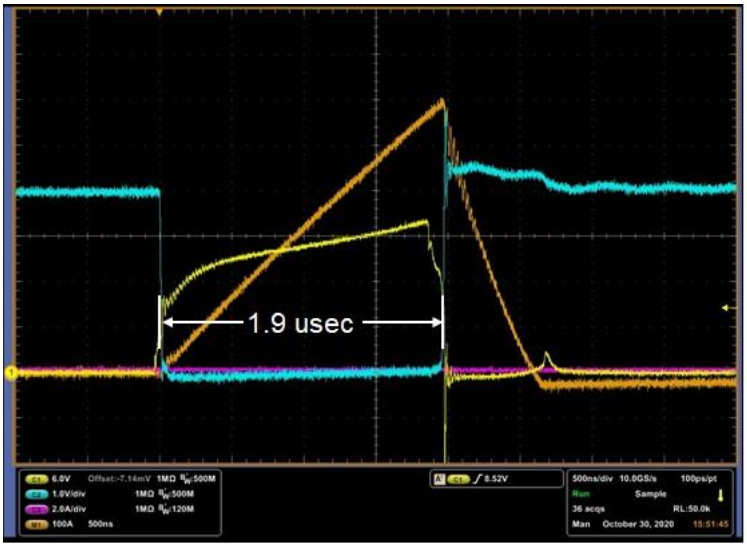


V_{in} : 230 V_{ac}/50 Hz (L, N, & PE), and P_{out} : 2.5 kW (400 V_{DC}, 6.25 A)

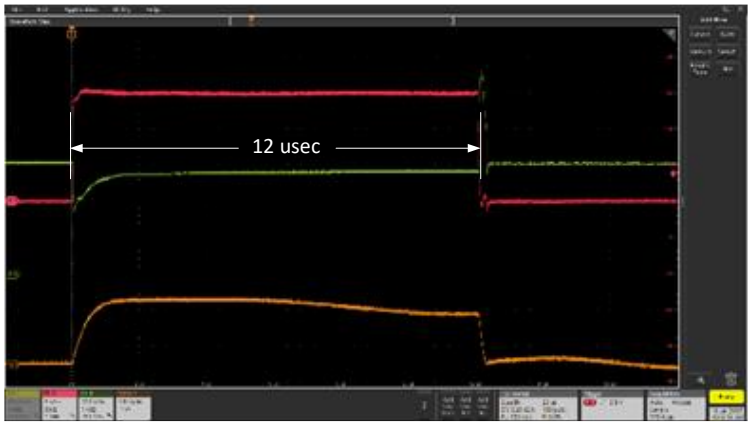
Figure 15 **EMI characteristics of IKW40N65WR5 and 80 mΩ CoolMOS™ P7 MOSFET with 20 A SiC diode combination @ f_{sw}=60 kHz**

4.4 SC immunity of IKW40N65WR5

The TRENCHSTOP™ 5 WR5 IGBT does not guarantee SCWT, but it can withstand the SC condition for a short period of time in practice because there is parasitic inductance around 1 ~ 2 µH existing in the PCB of PFC circuit. SC test waveforms of a conventional IGBT guaranteeing SCWT and IKW40N65WR5 are compared in Figure 16. As a result, IKW40N65WR5 withstands SC condition for 1.9 µsec, which can be sufficient to protect the IGBT when a proper over current protection circuit is applied.



(a) IKW40N65WR5



(b) IKW40N60H3

Figure 16 SC immunity of IKW40N65WR5 vs. a conventional SC rated IGBT, IKW40N60H3

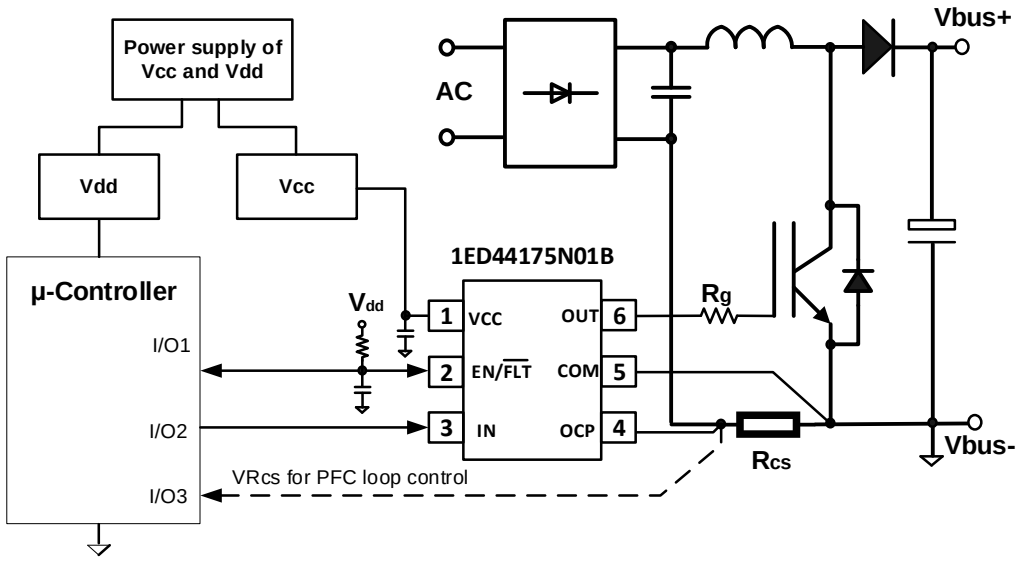
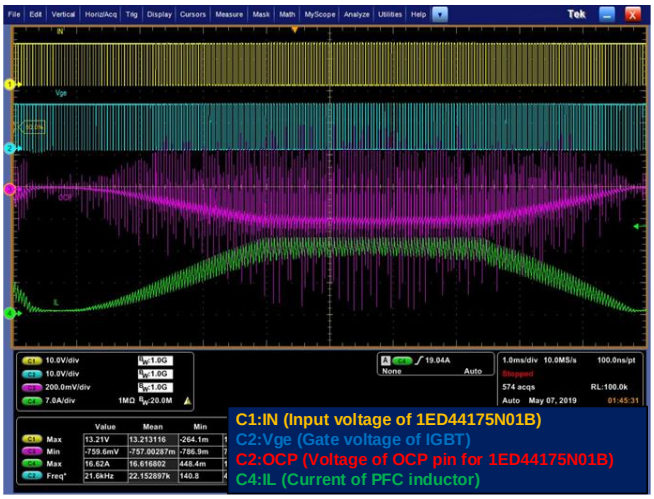
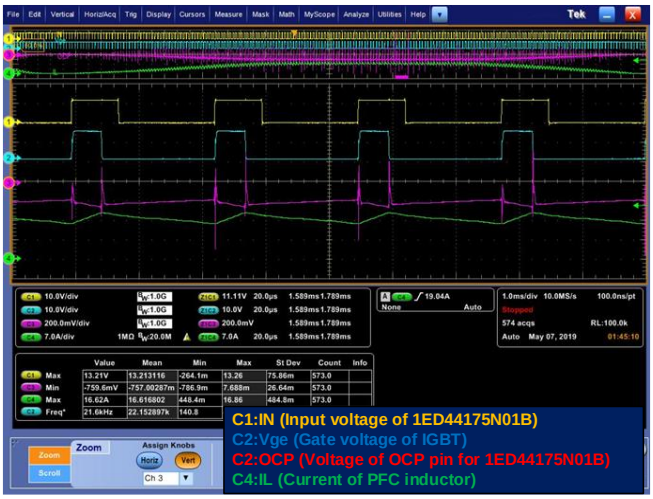


Figure 17 Example of an overcurrent protection by gate drive IC, 1ED44175N01B

Figure 17 indicates an example of an overcurrent protection circuit by gate drive IC (integrated circuit), 1ED44175N. In CCM PFC, a shunt resistor is generally required for average current mode control, and can also be used for overcurrent protection using the gate drive IC as shown in this Figure.



(a) Cycle by cycle OCP operation



(b) Zoomed in waveform

Figure 18 Cycle-by-cycle overcurrent protection by 1ED44175



- R_{g_on} = 27 Ω, R_{g_off} = 22 Ω
- External RC filter of OCP pin (330 Ω/1 nF)
- OCP delay time: T_{delay} < 500 nsec

Figure 19 PFC inductor SC test

Figure 18 shows a cycle-by-cycle OCP (overcurrent protection) test result using 1ED44175N in CCM PFC. The collect current of IGBT is limited to the certain OCP level, thereby the IGBT can be protected from overcurrent conditions. Figure 19 indicates a boost inductor SC test result that clearly shows the IGBT is protected within 1 µsec under the SC condition.

5 Conclusion

The validity of TRENCHSTOP™ 5 WR5 IGBT at CCM PFC circuit for major home appliances with high switching frequency up to 60 kHz was investigated and the performance comparison with a competitor's highest performing part and the equivalent CoolMOS™ P7 MOSFET was carried out. The results showed that the TRENCHSTOP™ 5 WR5 IGBT has far superior efficiency and thermal performance in high-frequency operation compared to the competitor's best performing part. At 60 kHz switching frequency, the TRENCHSTOP™ 5 WR5 IGBT showed 23°C lower temperature on the front side of PKG, and 0.34 % higher efficiency than the competitor's part. Compared to the equivalent CoolMOS™ P7 MOSFET, IKW40N65WR5 fared better in both efficiency and temperature characteristics at approximately 2 kW and above. In addition, the PKG temperature of TRENCHSTOP™ 5 WR5 IGBT at the switching frequency 60 kHz was 7°C lower than that of CoolMOS™ P7 MOSFET at the maximum power, 2.5 kW. TRENCHSTOP™ 5 WR5 IGBT also showed lower EMI levels than CoolMOS™ P7 MOSFET, which can be an additional merit. Lastly, even though TRENCHSTOP™ 5 WR5 IGBT is not a SC rated IGBT, it withstands SC conditions of more than 1 µsec. Therefore, this IGBT can be protected from the SC condition if the OCP response is fast enough. An OCP circuit using a fast-responding gate drive IC, 1ED44175N is proposed, and the validation results are also presented. Through the analysis results, it has been confirmed that TRENCHSTOP™ 5 WR5 IGBT is very suitable for PFC circuits for home-appliance applications where the performance of anti-parallel diodes is not important.

6 References

[1] E. M. Findlay and F. Udrea, "Reverse-Conducting Insulated Gate Bipolar Transistor: A Review of Current Technologies," in IEEE Transactions on Electron Devices, vol. 66, no. 1, pp. 219-231, Jan. 2019, doi: 10.1109/TED.2018.2882687.

[2] PFC boost converter design guide, Infineon Technologies AG, application note, Infineon Technologies AG, 2016

InfineonApplicationNote_PFCCCMBoostConverterDesignGuide-AN-v02_00-EN.pdf

[3] EVAL_2.5KW_CCM_4PIN, application note, Infineon Technologies AG, 2015

Infineon-ApplicationNote_EVAL_2.5KW_CCM_4PIN-ApplicationNotes-v01_00-EN.pdf

Revision history

Document version	Date of release	Description of changes
V1.0	2020-10-14	Initial version
V1.1	2020-12-09	Added complement description in Page 3
V1.2	2022-09-21	Corrected hold-up times on Page 4 Corrected the values in the tables on Page 11

Trademarks

All referenced product or service names amany

2020-12-09

Published by

Infineon Technologies AG

81726 Munich, Ger2022T 2020 Infineon Technologies AG.
All Rights Reserved.

Do you have a question about this document?

Email: erratum@infineon.com

Document reference

AN-2020-19 Number

IMPORTANT NOTICE

The information contained in this application note is given as a hint for the implementation of the product only and shall in no event be regarded as a description or warranty of a certain functionality, condition or quality of the product. Before implementation of the product, the recipient of this application note must verify any function and other technical information given herein in the real application. Infineon Technologies hereby disclaims any and all warranties and liabilities of any kind (including without limitation warranties of non-infringement of intellectual property rights of any third party) with respect to any and all information given in this application note.

The data contained in this document is exclusively intended for technically trained staff. It is the responsibility of customer's technical departments to evaluate the suitability of the product for the intended application and the completeness of the product information given in this document with respect to such application.

For further information on the product, technology, delivery terms and conditions and prices please contact your nearest Infineon Technologies office (**www.infineon.com**).

Please note that this product is not qualified according to the AEC Q100 or AEC Q101 documents of the Automotive Electronics Council.

WARNINGS

Due to technical requirements products may contain dangerous substances. For information on the types in question please contact your nearest Infineon Technologies office.

Except as otherwise explicitly approved by Infineon Technologies in a written document signed by authorized representatives of Infineon Technologies, Infineon Technologies' products may not be used in any applications where a failure of the product or any consequences of the use thereof can reasonably be expected to result in personal injury.